Molecular dynamics of collisions between rough surfaces

F. Delogu*
Dipartimento di Ingegneria Chimica e Materiali, Università degli Studi di Cagliari, piazza d'Armi, I-09123 Cagliari, Italy
(Received 13 September 2010; published 10 November 2010)

Classical molecular-dynamics simulations were carried out to investigate the collisions between two Ni crystals with rough surfaces at relative velocities in the range between 1 and 100 nm ns^{-1}. The response of the colliding solids was studied by monitoring local kinetic and potential energies as well as local mechanical stresses. A local order parameter was also used to discriminate between solidlike and liquidlike dynamics. Computation results indicate that both temperature and stress increase with the relative collision velocity. Averaged for the atoms within directly interacting surface asperities, the average temperature can reach values as high as 6000 K, the average pressure can be as high as 13 GPa, and the average normal stress as high as 16 GPa. Individual atoms can attain local temperatures as high as 10 000 K and local normal stresses as large as 20 GPa, depending on the surface morphology.

DOI: 10.1103/PhysRevB.82.205415 PACS number(s): 68.35.Af, 68.35.Ct, 61.43.Dq

I. INTRODUCTION

It is well known that the application of nonhydrostatic stresses to solid phases gives rise to an unusual form of chemistry, generally referred to as mechanochemistry.[1–4] Such chemistry must be related to the response of crystalline lattices to mechanical deformation.[1–4] In fact, deformation imposes to solids a departure from thermodynamic equilibrium that increases as the deformation rate increases,[1–4] which results in a general enhancement of the chemical reactivity.[3,4] In this regard, both elastic and plastic deformations are effective, but most of the experimental evidences concern the plastic deformation regime such as the one underlying mechanical alloying.[1–5]

A point gradually emerging in mechanochemistry is that the observed chemical processes are not exclusively governed by lattice defects.[6] Rather, the enhancement of chemical reactivity is likely to depend on all of the stages accompanying deformation, i.e. the accumulation of local strain, the occurrence of atomic rearrangements, and the successive relaxation of local structures.[6] Along this line, mechanochemistry can be regarded as the consequence of both transient perturbations and irreversible modifications of the coordination shells of individual atoms produced by mechanical stresses and shock waves propagating through the crystalline lattices.[6]

At present, various indirect experimental and numerical evidences suggest that the conditions under which mechanochemical processes take place can be quite severe.[7–12] In particular, the enhanced chemical reactivity observed in solid-solid and solid-gas reactions can be ascribed to local excited states (LESs) of various nature and lifetime that form when free surfaces participate in collision and friction processes.[11,12] Such LESs can be regarded as transient-energy localizations involving surface asperities,[13] where mechanical energy concentrates whenever two rough surfaces undergo a collision. A detailed knowledge of the atomic-scale processes taking place at collision represents the necessary basis to suitably understand and possibly control the formation and reactivity of LESs. Yet, information on this issue is almost completely lacking.

Starting from such evidence, the present work attempts to investigate the properties of LESs generated at collision by using classical molecular-dynamics methods. To such aim, two Ni semi-infinite crystals (SICs) terminating with rough surfaces were pushed against each other at different velocities and their response studied. It will be shown that atoms belonging to LESs can occasionally experience extremely severe local conditions.

II. GENERAL COMPUTATIONAL OUTLINE

Calculations were carried out on Ni SICs terminating with a rough free surface. The choice of Ni is motivated by the availability of both a reliable interatomic potentials[13,14] and previous results.[13] Interactions were described by a semi-empirical tight-binding potential based on the second-moment approximation to the density of electronic states.[13–15] The potential parameter values were taken from literature.[14] Forces were computed within a cut-off radius r_{cut} roughly corresponding to the seventh shell of neighbors. These conditions permit to satisfactorily reproduce thermodynamic and mechanical properties.[7,14–16]

A relatively large system formed by about 240 000 atoms arranged in a face-centered-cubic $cF4$ lattice with volume of about $16 \times 16 \times 10$ nm^3 was initially generated. Atoms were arranged in a stacking along the z Cartesian direction of (001) square planes including roughly 4000 atoms. The system was enclosed by periodic boundary conditions (PBCs) along the x, y, and z Cartesian directions and relaxed for 0.4 ns in the NPT ensemble with number of atoms N, pressure P, and temperature T constant.[17] Calculations were carried out at zero pressure and 300 K. Temperature was kept constant with the Nosè-Hoover thermostat.[18] Possible shape changes in the elementary crystallographic cell were allowed by using the Parrinello-Rahman scheme.[19] Equations of motion were solved by employing a fifth-order predictor-corrector algorithm.[17] A time step equal to 2 fs was used. Potential energy and volume fluctuations indicated that the 0.4 ns time interval was sufficient to attain a satisfactory equilibration of the crystalline lattice.

Regarding the time step employed to solve the equations of motion, it must be noted that the 2 fs value was only used during the preparation of Ni SICs. In fact, the time step was reduced to 0.1 fs during the simulation of impact events between surfaces. Such short integration time is needed to obtain a reliable description of the dynamics of individual atoms experiencing the extreme temperature and mechanical-stress conditions arising during the energy localization phenomena at collision. Focusing on the instantaneous behavior of individual atoms is one of the scopes of the present work. As discussed in the following, this apparently small change in perspective respect to previous works actually determined a significant, and somewhat unexpected, gain in fundamental knowledge.

A. Preparation of SICs and simulation of collision processes

Although surface asperities can be created artificially,[20–22] calculations were carried out on SICs generated by fracture of bulk systems submitted to tensile stresses. As shown in previous work,[13] this permits to create surfaces with realistic roughness. Ni SICs were obtained in various stages starting from the large relaxed $16\times16\times10$ nm^3 Ni bulk system. First, two reservoir regions of seven atomic planes each were created along the z Cartesian direction at the bottom and top of the simulation cell. PBCs were left along the x and y Cartesian directions. In each reservoir, the atomic positions in the five outer atomic planes were fixed whereas the atoms in the remaining two planes were left free to move. Then, reservoirs were progressively displaced in opposite sense along the z Cartesian direction at a nominal relative velocity of 1 nm ns^{-1}. A linear-velocity profile with values progressively changing from −0.5 to +0.5 nm ns^{-1} was also given to the atomic planes between reservoirs to avoid undesired shock waves and promote the nucleation of a fracture approximately at the middle of the simulation cell. During this stage, the Nosè-Hoover thermostat was only applied to the two mobile atomic planes in the reservoirs to not perturb the fracture nucleation and propagation with its fictitious dynamics. A description of the simulated system is given in Fig. 1.

In all of the investigated cases, the free surfaces of the SICs obtained by fracture are relatively rich in asperities, which make the surface profile quite irregular. The situation is schematically described in Fig. 1. Different simulations yield different surface profiles but their roughness degree is roughly constant. Individual atoms and small clusters are ejected in the gas phase during the course of, or immediately after, the fracture process, as roughly depicted in Fig. 1. Being quite energetic, these species collide with the newly created free surfaces, further increasing their roughness.

The relative displacement of SICs was stopped at a distance between their surfaces of about 3 nm. Then, the SICs were kept at such distance and relaxed for time intervals on the order of 1–2 ns. During this time interval, almost all of the gas-phase species interact with the free surfaces and are absorbed. The remaining ones were eliminated.

Collisions were simulated by using SICs generated in different simulations to avoid complementary surface profiles. The initial configuration, schematically described in Fig. 2,

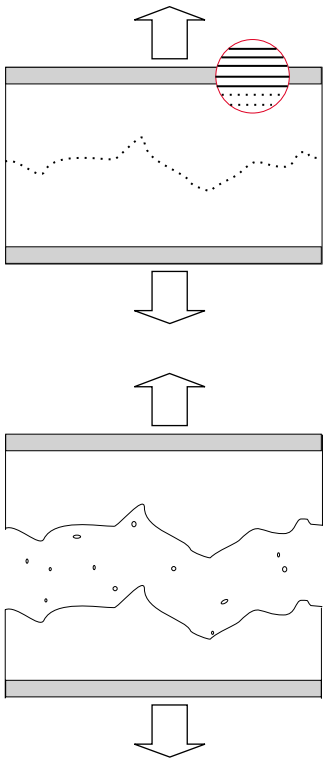

FIG. 1. (Color online) A schematic description of the system configuration before (top) and after (bottom) a fracture. The two reservoirs along the z Cartesian direction are shown in gray. A sketch of the reservoir structure is given in the circle to show the five rigid (solid line) and the two mobile (dotted line) atomic planes. Arrows indicate relative displacement directions whereas the dotted line between reservoirs roughly describes the fracture profile.

was created by placing the SICs in front of each other leaving a distance between the nearest atoms on opposite surfaces slightly longer than the potential cut-off radius r_{cut}. PBCs were applied along the x and y Cartesian directions. Then, a force was applied to rigid reservoirs to approach SICs along the z Cartesian direction. The force intensity was

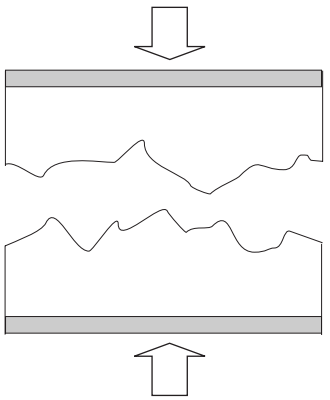

FIG. 2. A schematic description of the initial configuration used for collision processes. The two reservoirs along the z Cartesian direction are shown in gray. Arrows indicate the relative displacement along the z Cartesian direction.

suitably adjusted to produce nominal relative collision velocities v_{imp} in the range between 1 and 100 nm ns^{-1}. Forces were maintained also after the collision to produce compressive uniaxial strains preventing the separation of SICs. For simplicity, no rotational degree of freedom was given to reservoirs. As a consequence, SICs were allowed to move relative to each other only by keeping their reservoirs parallel.

It must be noted that both PBCs and reservoirs could, in principle, affect the system dynamics. In fact, local stress fields at the points of contact between surface asperities determine the nucleation and migration of dislocations, which could, however, be stopped precisely by rigid reservoirs. Also, a given dislocation could interact with its virtual image created by PBCs. Fortunately, as detailed in previous work,[13] SICs are large enough to make PBCs and reservoirs effects negligible. In addition, it must be kept in mind that the work focuses on the behavior of atoms involved in LESs, which generally are not affected by dislocation dynamics because of melting phenomena.

B. Characterization of LESs

LESs were identified by looking at the kinetic energy E of any given atom. In particular, a given atom was regarded as belonging to a LES when its kinetic energy E was higher than a threshold value E_0. Based on previous work,[13] a E_0 value of about 6 kJ mol^{-1} was used. At 300 K, such energy is possessed by only the 0.5% of atoms in the system.

The number N_{LES} of LESs was evaluated starting from the evidence that excited atoms usually form connected clusters.[13] Two excited atoms were regarded as connected in the same cluster if they were nearest neighbors, i.e., if located at a distance shorter than $r_{\mathbf{min}}$, the distance at which the Ni pair-distribution function exhibits its first minimum. This simple distance criterion allows to evaluate the instantaneous number n_{LES} of excited atoms in any given LES, which, in turn, permits to quantify the number N_{LES} of individual LESs.

Aimed at suitably identifying possible local melting phenomena and distinguishing between solidlike and liquidlike dynamics, a local order parameter depending on the configuration of nearest neighbors was defined for each atom. Following previous work,[20,21] a set of N_q wave vectors q such that $e^{i\boldsymbol{q}\cdot\boldsymbol{r}}=1$ was selected for any vector r connecting a pair of nearest neighbors in a perfect fcc lattice. One of the two antiparallel r vectors connecting a given atom pair was, however, discarded so that N_q was equal to 6. The local order parameter was then defined as

$$\psi_i = \left| \frac{1}{N_q z} \sum_{\boldsymbol{r}} \sum_{\boldsymbol{q}} e^{i\boldsymbol{q}\cdot\boldsymbol{r}} \right|^2, \tag{1}$$

where the sum on r vectors runs over the z nearest neighbors of the atom i. Nearest neighbors are here defined as any two atoms located at distances smaller than $r_{\mathbf{min}}$. The local order parameter ψ_i is equal to 1 for any atom in a perfect fcc lattice site and smaller otherwise.[20,21] Then, it can be used to distinguish solid-phase atoms from liquid-phase ones. However, such discrimination can be improved by working on suitably averaged atomic positions and taking into account the degree of order of nearest neighbors. Indeed, instantaneous atomic positions are affected by fast thermal vibrations and the instantaneous degree of order of a given atomic configuration is correspondingly decreased. The order parameter ψ_i was accordingly evaluated on atomic positions averaged over 5 ps and an average local order parameter was defined as[20,21]

$$\overline{\psi_i} = \frac{1}{z+1}\left(\psi_i + \sum_j \psi_j\right), \tag{2}$$

where j runs over the z nearest neighbors of the atom i. Atoms in a liquid region are characterized by $\overline{\psi_i}$ values smaller than 0.05 whereas the solid phase includes atomic species with $\overline{\psi_i}$ values larger than 0.2.[20,21] In addition, only a few atoms located at the solid-liquid interface possess $\overline{\psi_i}$ values between the aforementioned thresholds.[20,21] In the following, atoms with $\overline{\psi_i}$ values smaller than 0.08 will be defined as liquidlike and the remaining ones as solidlike.

The local atomic stress was estimated by calculating the local stress tensor β^i_{km}. This was evaluated for each atom i according to the expression[22]

$$\beta^i_{\mathrm{km}} = \frac{1}{\Omega^i} \sum_{j\neq i}^{N_{nn}} f^{ij}_{\mathrm{k}} r^{ij}_{\mathrm{m}}, \tag{3}$$

where Ω^i is the atomic volume, $\boldsymbol{f}^{ij}_{\mathrm{k}}$ and $\boldsymbol{r}^{ij}_{\mathrm{k}}$ are, respectively, the force and the position vectors connecting the atoms i and j, and N_{nn} is the number of nearest neighbors of atom i. The stress tensor β^i_{km} was used to estimate the average pressure P_{LES} and the average normal stress σ_{LES} within each LES by averaging over the number n_{LES} of atoms in the selected LES. The atomic volume Ω^i was estimated by tessellating the space with Voronoi polyhedra.[23,24] More specifically, Voronoi polyhedra were defined around each atom and their volume evaluated according to standard numerical methods.

Regarding surface processes at collision, it is worth noting that the systems employed in computations have a nominal surface area of only 16×16 nm^2. Although this value can be considered relatively large in connection with the cumbersome calculations carried out, it is nevertheless quite small with reference to realistic situations. Previous work has shown that 16×16 nm^2 exhibit only two to four significant asperities.[13] It follows that each simulation permits to analyze the dynamics of only two to four points of impact between the colliding solids, very small numbers compared with real phenomena. Here, such limitation has been partly tackled by performing ten different simulations per each relative collision velocity v_{imp} value. As a whole, about 100 different simulations have been carried out to investigate the collision dynamics and the consequent formation and evolution of LESs. Even though the conceptual framework obtained is still quite fragmentary, the numerical findings provide a first clue to the complex sequence of processes taking place at the collision between two solid phases.

As a final comment, it must be noted that, in contrast with previous work,[13] the analysis of LESs was not restricted to surface regions but extended to bulk ones. This required more cumbersome calculations, due to the larger number of atoms to deal with.

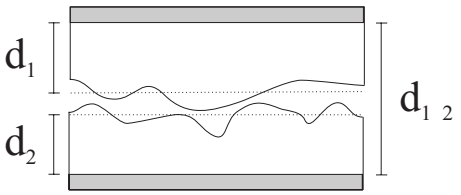

FIG. 3. A schematic description of the system with the distance d_{12} between reservoirs and the distances d_1 and d_2 of the average surfaces (dotted horizontal lines) of the Ni SICs 1 and 2 from their reservoirs.

III. RESULTS AND DISCUSSION

Collision processes were monitored by evaluating the average distance d between the surfaces of Ni SICs as a function of time t. The distance d is defined as the difference $d_{12}-d_1-d_2$. Here, d_i represents the average distance of the surface of the ith Ni SIC from its reservoir and was evaluated by averaging over the z Cartesian coordinates of all of the surface atoms. Instead, d_{12} is the distance between the reservoirs. The different quantities are schematically indicated in Fig. 3. The d and d_{12} values are shown in Fig. 4 as a function of time t for two SICs colliding at different relative velocity v_{imp}. It can be seen that both d and d_{12} undergo a roughly linear decrease until surface asperities come into contact, i.e., until the first atoms on opposite surfaces start interacting with repulsive forces. As this occurs, the slopes of d and d_{12} plots change. However, whereas shortly after the first contact d fluctuates irregularly around an average value, d_{12} gradually reaches an asymptotic value with negligible fluctuations.

The behavior of d and d_{12} originates from the application of compressive forces to the reservoirs of Ni SICs. The uniaxial stress pushing the surfaces against each other drives the two Ni SICs toward a complete adhesion. During the first stages of the collision event, adhesion is contrasted by the intense repulsive forces arising from the contact between surface asperities. Precisely such forces are responsible for the nucleation of defects, in particular, of dislocations, that

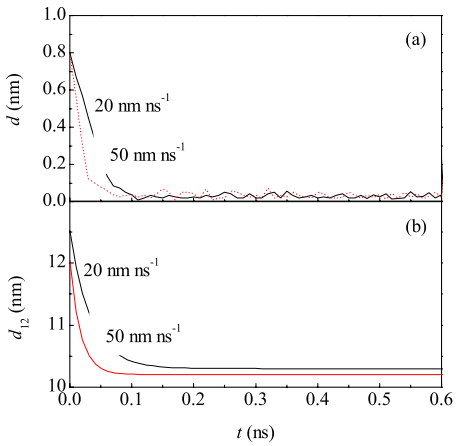

FIG. 4. (Color online) (a) The distance d between the surfaces of the Ni SICs and (b) the distance d_{12} between their reservoirs as a function of time t. Data refer to Ni SICs impacting at the relative collision velocity v_{imp} values indicated.

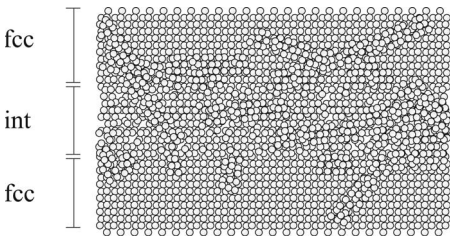

FIG. 5. A portion of the system obtained after collision and compression of two Ni SICs initially approaching at a relative collision velocity v_{imp} of 20 nm ns^{-1}. For clarity, the atoms belonging to different fcc defective domains (fcc) and to the disordered interface (int) SICs are indicated.

gradually modify surface profiles. In turn, this permits the approach of Ni SICs to shorter distances and secondarily produces the reduction in the amplitude of d fluctuations.

In all of the investigated cases, the final asymptotic value reached by the distance d_{12} between reservoirs is quite close to the one obtained by approaching two Ni SICs with the same number of atoms of colliding ones but arranged to form plane surfaces. In fact, the collision and the successive compression of SICs finally results in the formation of a single Ni crystal with a disordered interface separating two ordered fcc domains, as shown in Fig. 5 for the system formed by collision of two SICs moving at 20 nm ns^{-1}. Therefore, the final density is close to the one of a nanocrystalline phase. Of course, the evolution of the interface during and after the collision between SICs is affected by the constraint of keeping the reservoirs parallel. Nevertheless, the obtainment of a single phase with a thin disordered region approximately in the middle points out the occurrence of welding phenomena. Regarding this latter point, further indications come from the evaluation of the solidlike or liquidlike character of atoms based on the values of the average local order parameter $\overline{\psi_i}$. Data concerning the first six atoms involved in repulsive forces on both sides of SICs colliding at a relative velocity v_{imp} of 50 nm ns^{-1} are shown in Fig. 6 as a function of time t. It can be seen that, for each atom, $\overline{\psi_i}$ undergoes an extremely fast decrease from the initial value to about 0 on time scales on the order of 1 ps. Of course, the initial $\overline{\psi_i}$ values are far from 1, which is the value expected for atoms located in a perfect crystalline lattice at 0 K. In fact, the atoms experiencing the first contact between the colliding SICs are located at surface asperities, and then have a num-

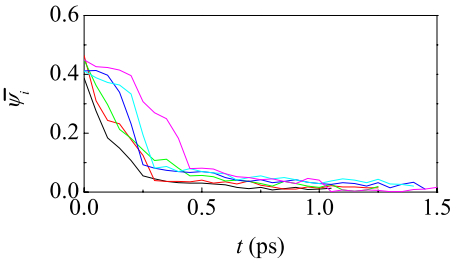

FIG. 6. (Color online) The average local order parameter $\overline{\psi_i}$ as a function of time t. Data concern the first six atoms involved in repulsive forces on both sides of Ni SICs colliding at a relative velocity v_{imp} of 50 nm ns^{-1}.

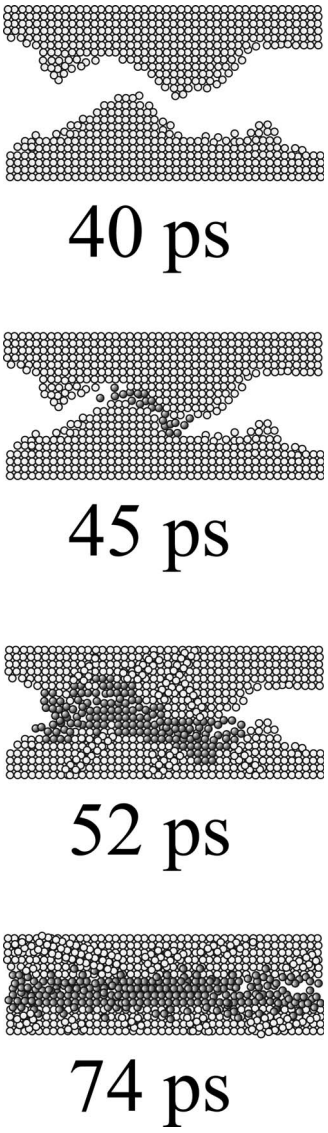

FIG. 7. Liquidlike atoms present in the atomic configurations of SICs colliding at a relative velocity v_{imp} of 20 nm ns^{-1}. Data refer to portions of atomic configurations taken after the indicated time intervals from the beginning of calculations. Liquidlike atoms are shown in dark gray.

ber of nearest neighbors smaller than the equilibrium one. It follows that these surface atoms have a dynamics significantly more disordered than bulk ones. In spite of this, the monitored atoms initially exhibit a solidlike dynamics with $\overline{\psi}_i$ values well above the threshold of 0.05 that identifies the liquidlike behavior. Similar results are found when different systems and larger sets of atoms are considered.

The fast attainment of a liquidlike dynamics is a consequence of energy localization processes taking place at collision. Initially, the impact is substantially sustained by the surface asperities come into contact. Already at this stage, crystalline lattice defects such as vacancies, interstitials, and dislocations nucleate and propagate. However, the system dynamics rapidly becomes so complex and energetic that a detailed analysis of defect dynamics is not possible. Such analysis can be replaced by a more general, and at the same

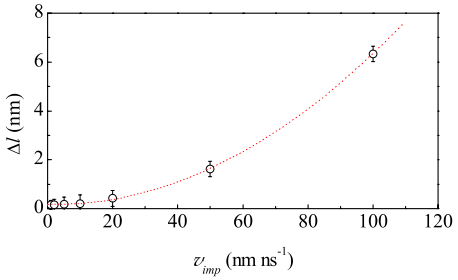

FIG. 8. (Color online) The maximum thickness Δl reached by the liquidlike layer as a function of the relative collision velocity v_{imp}. Error bars account for the Δl values obtained in different simulations. The best-fitted quadratic curve is also shown.

time rougher, evaluation of energy flows through the visualization of atoms with liquidlike dynamics. An example of the information obtained is given in Fig. 7, where the liquidlike atoms of colliding SICs are shown at different time intervals from the beginning of the impact. It can be seen that the liquidlike behavior is initially strongly localized at the first points of contact between surface asperities. Then, the kinetic energy rapidly spreads in the neighborhood of such points, determining the appearance of an increasingly large number of atoms exhibiting liquidlike dynamics. After a relatively short-time interval from the beginning of impact, which depends on the relative collision velocity v_{imp}, the liquidlike dynamics has spread over the whole surface region, also involving the atoms located about 0.7 nm below the free surface. Of course, it is precisely during this stage that surface profiles undergo the deepest modifications with liquidlike atoms rapidly displacing in the attempt of lowering their energy. After sufficient time has elapsed, an almost homogeneous liquid layer is observed at the interface between the domains in which Ni atoms have kept their initial solidlike behavior. Finally, the slow dissipation of kinetic energy operated by the thermostat applied to the mobile atoms in the reservoirs allows liquidlike atoms to gain back a solidlike dynamics.

The maximum thickness Δl reached by the layer of atoms with liquidlike dynamics depends on the relative collision velocity v_{imp}. The relationship between these two quantities is pointed out in Fig. 8, where Δl is shown as a function of v_{imp}. The plot is approximately quadratic. Accordingly, it can be inferred that the maximum thickness Δl reached by the layer is dominated by the total energy deposited at the interface, the thermostat being able to remove effectively the excess energy only at lower energies.

Similar inferences can be drawn by monitoring the total number n_{liq} of atoms with liquidlike dynamics. The n_{liq} data sets concerning Ni SICs collision at different relative velocity v_{imp}, not shown for brevity, point out that n_{liq} undergoes a sudden increase, followed by the attainment of a roughly constant value. Such constant value is kept for time intervals the length of which increases with the relative collision velocity v_{imp}. Afterward, a much slower decrease is observed due to the dissipation of kinetic energy operated by the thermostat.

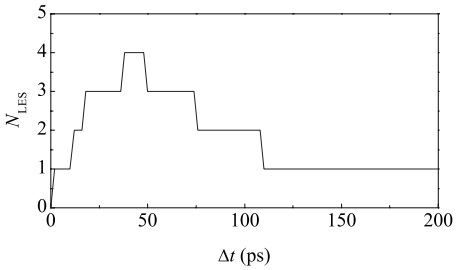

FIG. 9. The number N_{LES} of individual LESs as a function of time t. Data refer to the case of two Ni SICs colliding at a relative velocity v_{imp} of 10 nm ns^{-1}.

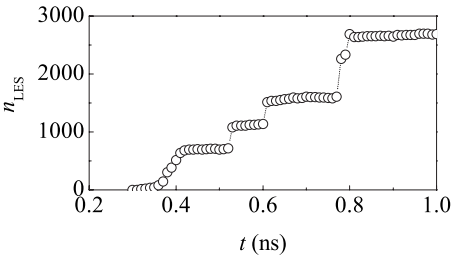

FIG. 10. The number n_{LES} of atoms connected in an individual LES as a function of time t. Data refer to the case of Ni SICs colliding at a relative velocity v_{imp} of 20 nm ns^{-1}.

The results heretofore presented indicate that the collision and subsequent compression of Ni SICs induce a general excitation of surface regions, determining first their melting and then the welding of colliding SICs, with the formation of a disordered interface between the ordered Ni domains. Although studied on a different level, the situation is clearly reminiscent of the one predicted on a theoretical basis for mechanochemical transformations. In fact, previous studies already suggested that the localization of energy in mechanically activated transformations could take place according to the mechanism referred to as "virtual melting."[25,26] In particular, the energy connected with local stresses is expected to increase the driving force for melting, reducing the melting point.[25,26] Stresses relax as melting occurs, and the unstable melt immediately solidifies, with no effect on the thermodynamics and the kinetics of the solid-solid phase transformation occurred.[25,26] The numerical evidences obtained seem to perfectly fit this scenario, even though the time scale explored does not allow to observe the solidification processes subsequent to melting.

After a certain time has elapsed from the beginning of the impact, all of the atoms initially located at, or in the neighborhood of, free surfaces exhibit a kinetic energy E considerably higher than bulk atoms. However, the attainment of such general excited state passes through a sequence of local events that determine the formation and evolution of various LESs. On the average, the number N_{LES} of individual LESs changes with time t as shown in Fig. 9. Initially, it rises from 0 to 3, 4, and 5 depending on the number and morphology of the surface asperities of Ni SICs. Afterward, N_{LES} decreases quite rapidly to 1. Data in Fig. 9 refer to the case of Ni SICs colliding at a relative velocity v_{imp} equal to 10 nm ns^{-1}, but similar results are obtained in the other cases. The time scale over which N_{LES} changes depends on the relative collision velocity v_{imp}, the overall variation in N_{LES} being faster for higher v_{imp} values. Instead, the details of N_{LES} variation depend on the surface morphology.

The N_{LES} behavior observed in all of the investigated cases originates from the variation in the size n_{LES} of individual LESs with time t as collision and compression processes take place. In fact, as individual LESs grow, they finally connect in a single excited domain extending to all of the surface regions. A typical variation in the number n_{LES} of atoms connected in individual LESs is shown in Fig. 10, where n_{LES} is plotted as a function of time t. Various stages in the growth of the considered LES can be identified. First, the LES undergoes a relatively slow progressive growth with n_{LES} increasing gradually according to a roughly sigmoidal trend. Then, sudden rises are observed superposed to a constant growth due to the coalescence between neighboring LESs. Data in Fig. 10 refer to the case of Ni SICs colliding at a relative velocity v_{imp} of 20 nm ns^{-1} but the behavior observed is well representative of other cases.

The results coming from the ten different simulations per relative collision velocity v_{imp} value can be suitably combined to work out a few interesting quantities such as the average temperature T_{LES}, potential energy U_{LES}, pressure P_{LES}, and local atomic normal stress σ_{LES} exhibited by individual LESs. To evaluate the mentioned quantities, only isolated LESs were considered. Therefore, the study of a given LES was interrupted as soon as it became connected with a neighboring LES. It follows that the quantities T_{LES}, U_{LES}, P_{LES}, and σ_{LES} necessarily focus on the first stages of the collision. Their average values are shown in Fig. 11 as a function of time t. All of the quantities initially increase, then reach a maximum value and finally decrease. The maximum values are reached approximately at the same time, even though with different rates. The final decreases also take place at different rates.

The behavior of different LESs can be tentatively described in terms of characteristic quantities averaged over the ten simulations carried out per relative collision velocity v_{imp} value. Such quantities are the average maximum LES temperature $\langle T_{LES} \rangle$, the average maximum LES potential energy $\langle U_{LES} \rangle$, the average maximum pressure $\langle P_{LES} \rangle$, and the average maximum local atomic normal stress $\langle \sigma_{LES} \rangle$. These quantities are shown in Fig. 12 as a function of the relative collision velocity v_{imp}. Data indicate that all of the considered quantities increase with v_{imp} according to different trends. Very large $\langle T_{LES} \rangle$ values are reached, in the range between 1200 and 6000 K. Quite reasonably, the highest average maximum temperatures $\langle T_{LES} \rangle$ is attained in correspondence of the highest relative collision velocity v_{imp}. Similar considerations can be made for the potential energy $\langle U_{LES} \rangle$, the pressure $\langle P_{LES} \rangle$, and the normal stress $\langle \sigma_{LES} \rangle$. However, the former quantity increases according to a linear trend whereas the latter ones exhibit a growth roughly complementary to an exponential decrease.

More surprising evidences are obtained when the behavior of individual atoms is studied in detail. In fact, small

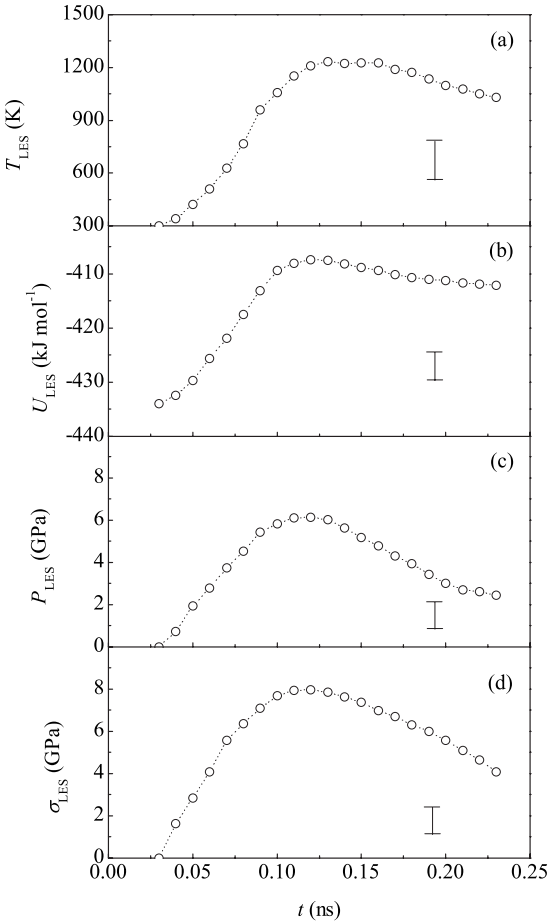

FIG. 11. (a) The average temperature T_{LES}, (b) potential energy U_{LES}, (c) pressure P_{LES}, and (d) local atomic normal stress σ_{LES} exhibited by a LES as a function of time t. Data refer to the case of Ni SICs colliding at a relative velocity v_{imp} of 2 nm ns^{-1}. For clarity, average error bars regarding data at times t longer than 0.1 ns are shown separately.

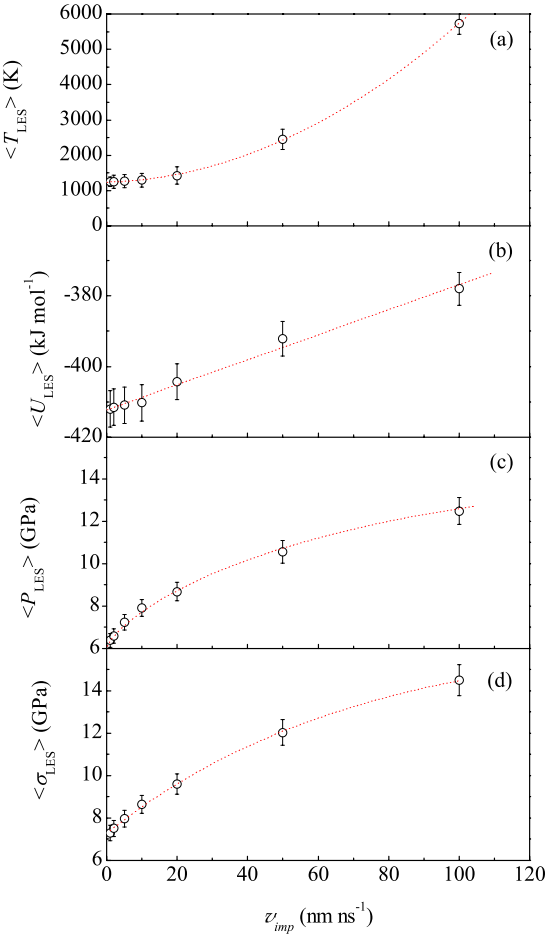

FIG. 12. (Color online) (a) The average maximum LES temperature $\langle T_{LES} \rangle$, (b) the average maximum LES potential energy $\langle U_{LES} \rangle$, (c) the average maximum LES pressure $\langle P_{LES} \rangle$, and (d) the average maximum local atomic normal stress $\langle \sigma_{LES} \rangle$ as a function of the relative collision velocity v_{imp}. Error bars account for values obtained in different simulations. Best-fitted curves are also shown.

groups of two to five atoms are occasionally observed to reach instantaneous temperatures T_k, pressures P_k, and normal stresses σ_k as high as 6400 K, 12 GPa, and 15 GPa, respectively. A typical example is shown in Fig. 13 for an individual atom involved in the very first stages of a LES formation. It can be seen that T_k reaches a maximum value roughly equal to 9430 K in about 80 fs and keeps higher than 5000 K for about 1 ps. According to thermodynamics, at such temperatures Ni atoms are in vapor phase.[27] However, in the present case evaporation processes are prevented by the confinement effect due to the collision of free surfaces and the following compression stage, which result in the extremely large instantaneous values of pressure P_k and normal stress σ_k. These observations clearly indicate that a few atoms among all of the ones forming LESs can attain extreme temperature and stress conditions. Similar evidences have been obtained for high-energy cluster impact and erosion processes at the surface of solids.[28,29] Temperatures and stresses as high as 1×10^4–1×10^5 K and 1–10 GPa have been observed.[28,29]

Interestingly, the observed T_k, P_k, and σ_k values are not trivially connected with the relative velocity v_{imp} at which Ni SICs collide. In fact, extremely energetic atoms with similar properties and behavior are identified with roughly the same probability in SICs colliding at 1 or 100 nm ns^{-1}. This suggests that the attainment of such extreme conditions could be related to the morphology of the surface and, in particular, to the presence of specific features that allow the localization of large amounts of kinetic energy at impact and prevent the evaporation of the atoms involved.

To check the validity of such conjecture, additional simulations were carried out on suitably prepared idealized systems. Two Ni SICs were created, respectively, with a pyramidal outward asperity and a pyramidal hole at the center of the free surface. Asperity and hole were given the same position and their sides the same slope. Instead, their heights were given different values so that the tip of the pyramidal asperity comes into contact with the bottom of the pyramidal hole when the plane portions of the SIC surfaces are still about 1 nm far apart. The profiles of the two Ni SICs employed are shown in Fig. 14.

The two above-mentioned Ni SICs were submitted to collision at both 1 and 100 nm ns^{-1}. In the first case, six atoms

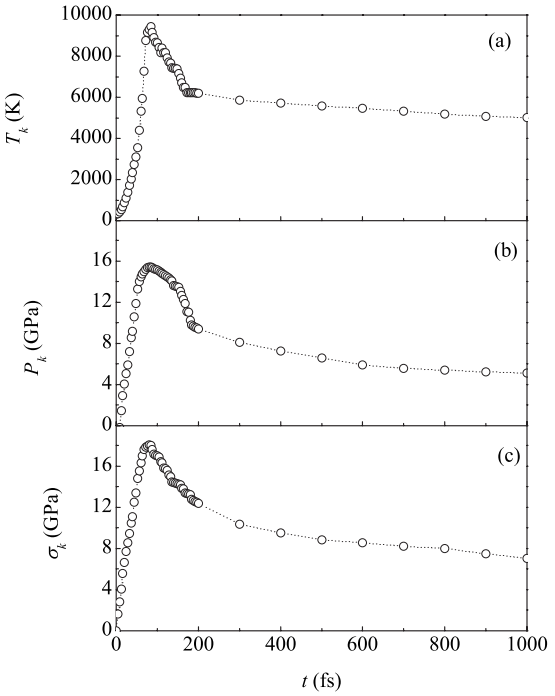

FIG. 13. (a) The instantaneous temperature T_k, (b) pressure P_k and normal stress σ_k as a function of time t. Data refer to the case of an individual atom involved in the very first stages of LES formation for Ni SICs colliding at a relative velocity v_{imp} of 5 nm ns^{-1}.

initially at the tip of the pyramidal asperity and four at the bottom of the pyramidal hole have been able to reach individual temperatures T_k as high as 10 500 K. In the second case, similar temperatures T_k were attained, but by 18 atoms. In both cases, the maximum instantaneous normal stress σ_k values were as large as 19 GPa. Therefore, it seems that the relative collision velocity v_{imp} affects the total number of atoms involved in the energy-localization processes, which becomes slightly larger as the collision velocity increases, but not the maximum temperatures attained. Regarding these, it must be noted that the very large T_k values, in combination with the very large P_k and σ_k values, are compatible with the local formation of a plasma.[30,31] In turn, this reminds to the first observations concerning tribological emissions from fractured and energetically rubbed solid surfaces.[1,2] Should these numerical evidences be supported by experimental findings, a very interesting avenue of research would open in the field of mechanochemistry.

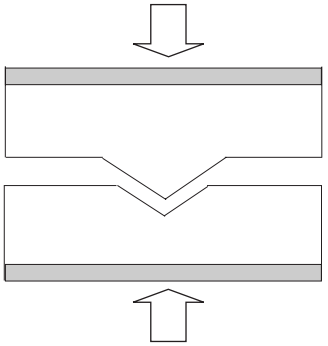

FIG. 14. A schematic description of the initial configuration used for the collision processes. The two reservoirs along the z Cartesian direction are shown in gray. Arrows indicate the displacement along the z Cartesian direction.

As a final comment on the above-mentioned numerical findings, it must be here noted that the results obtained can be considered at best rough approximations of real situations. In fact, the attainment of physical conditions as severe as the ones generically suggested by simulations precludes any physically meaningful description by classical many-body potentials. The very high temperatures and mechanical stresses locally reached by the atoms involved in the first contacts at the surface asperities readily suggest that ionization processes could take place. Correspondingly, the appearance of charged species in connection with the rapid evolution of local electric and magnetic fields determines a deep modification of the system physics, no longer amenable to be described by effective potentials.[17] At the same time, *ab initio* methods are far from any possible application to such physical problem, being the system characterized by a extremely fast evolution of properties.[32,33] Nevertheless, the results obtained in the present investigation have the merit of pointing out the need of studying in deeper detail the phenomenology connected with mechanochemical transformations, once more calling the attention on local phenomena that could easily provide invaluable examples of unusual physical behavior.

IV. CONCLUSIONS

The results of classical molecular-dynamics simulations indicate that local atomic rearrangement processes occurring at the collision between two rough surfaces can take place under very severe energetic conditions. Nonhydrostatic mechanical stresses develop at the points of contact between surface asperities, where mechanical energy is initially dissipated. The consequent formation and growth of LESs is characterized by a considerable increase in local temperature, potential energy, and stress. In turn, this determines the melting of the surface layer and the appearance of an approximately homogeneous layer of atoms with liquidlike dynamics. Together with the dissipation of excess kinetic energy, the compression of Ni SICs against each other finally allows the formation of a disordered interface between two defective crystalline domains.

Regarding LESs, numerical findings support previous results.[13] On the average, local temperatures and stresses depend on the relative collision velocity between Ni SICs, although surface roughness and morphology have a significant influence on local events. Temperature exhibits a quadratic dependence on the relative collision velocity, which suggests that local heating is strictly connected with the kinetic energy dissipated at collision. Instead, potential energy and local stress undergo a more complex behavior, probably due to their dependence on the detail of local atomic rearrangements. As a whole, LESs can attain tem-

peratures as high as 6000 K as well as pressures and stresses as large as 13 GPa and 16 GPa, respectively. However, individual atoms can occasionally attain temperature, pressure, and stress values on the order of 10 000 K, 17 GPa, and 20 GPa, almost irrespective of the initial relative collision velocity.

ACKNOWLEDGMENTS

Financial support has been provided by the University of Sassari and the University of Cagliari. A. Ermini, ExtraInformatica s.r.l., is gratefully acknowledged for the technical support.

*delogu@dicm.unica.it

[1] G. Heinicke, *Tribochemistry* (Akademie-Verlag, Berlin, 1984).
[2] P. Yu. Butyagin, Sov. Sci. Rev. B Chem. **14**, 1 (1989).
[3] E. M. Gutman, *Mechanochemistry of Materials* (Cambridge International Science, Cambridge, 1998).
[4] V. I. Levitas, in *High Pressure Surface Science and Engineering*, edited by Y. Gogotsi and V. Domnich (Institute of Physics, Bristol, 2004), Chap. 3, p. 159.
[5] C. Suryanarayana, Prog. Mater. Sci. **46**, 1 (2001).
[6] *Experimental and Theoretical Studies in Modern Mechanochemistry*, edited by F. Delogu and G. Mulas (Transworld Research Network, Kerala, India, 2010).
[7] F. Delogu and G. Cocco, Phys. Rev. B **72**, 014124 (2005).
[8] F. Delogu, J. Appl. Phys. **104**, 073533 (2008).
[9] F. Delogu, Scr. Mater. **58**, 126 (2008).
[10] G. Mulas, F. Delogu, C. Pistidda, and G. Cocco, J. Mater. Sci. **43**, 5193 (2008).
[11] F. Delogu and G. Mulas, Int. J. Hydrogen Energy **34**, 3026 (2009).
[12] F. Delogu, G. Mulas, and S. Garroni, Appl. Catal., A **366**, 201 (2009).
[13] F. Delogu, Phys. Rev. B **80**, 014115 (2009).
[14] F. Cleri and V. Rosato, Phys. Rev. B **48**, 22 (1993).
[15] F. Ducastelle, J. Phys. (Paris) **31**, 1055 (1970).
[16] V. Rosato, M. Guillope, and B. Legrand, Philos. Mag. A **59**, 321 (1989).
[17] M. P. Allen and D. Tildesley, *Computer Simulation of Liquids* (Clarendon Press, Oxford, UK, 1987).
[18] S. Nosè, J. Chem. Phys. **81**, 511 (1984).
[19] M. Parrinello and A. Rahman, J. Appl. Phys. **52**, 7182 (1981).
[20] J. R. Morris, Phys. Rev. B **66**, 144104 (2002).
[21] J. R. Morris and X. Song, J. Chem. Phys. **116**, 9352 (2002).
[22] M. F. Horstemeyer, M. I. Baskes, and S. J. Plimpton, Theor. Appl. Fract. Mech. **37**, 49 (2001).
[23] G. F. Voronoi, J. Reine Angew. Math. **134**, 198 (1908).
[24] J. L. Finney, Proc. R. Soc. London, Ser. A **319**, 495 (1970).
[25] V. I. Levitas, B. F. Henson, L. B. Smilowitz, and B. W. Asay, Phys. Rev. Lett. **92**, 235702 (2004).
[26] V. I. Levitas, Phys. Rev. Lett. **95**, 075701 (2005).
[27] *Smithells Metals Reference Handbook*, 7th ed., edited by E. A. Brandes and G. B. Brook (Butterworth-Heinemann, Oxford, 1992).
[28] Y. Yamaguchi and J. Gspann, Phys. Rev. B **66**, 155408 (2002).
[29] V. N. Popok and E. E. B. Campbell, Rev. Adv. Mater. Sci. **11**, 19 (2006).
[30] F. F. Chen, *Introduction to Plasma Physics and Controlled Fusion* (Springer, New York, 1984).
[31] *Plasma Physics*, edited by R. O. Dendy (Cambridge University Press, Cambridge, 1993).
[32] D. Marx and J. Hutter, *Modern Methods and Algorithms of Quantum Chemistry*, NIC Series Vol. 1, edited by J. Grotendorst (John von Neumann Institute for Computing, Jülich, 2000), p. 301.
[33] R. Iftimie, P. Minary, and M. E. Tuckerman, Proc. Natl. Acad. Sci. U.S.A. **102**, 6654 (2005).